

Received September 20, 2021, accepted October 3, 2021, date of publication October 8, 2021, date of current version October 18, 2021.

Digital Object Identifier 10.1109/ACCESS.2021.3118686

# 5G Wireless Emergency Alerts Based on Image Code and Cell Clustering

SEKCHIN CHANG 

Department of Electrical and Computer Engineering, University of Seoul, Seoul 02504, Republic of Korea

e-mail: schang213@uos.ac.kr

This work was supported by the Research Program through the National Research Foundation of Korea (NRF) under Grant 2017R1A2B4005105.

**ABSTRACT** This paper addresses novel wireless emergency alerts based on image code and cell clustering in 5G cellular systems. Most cellular systems offer a cell broadcast technique for emergency alert delivery. The cell broadcast method simultaneously delivers text-based messages to the users in specific cells, which encompass emergency areas. For the simultaneous delivery, the cell broadcast approach relies on a broadcast mechanism, which is called cell broadcast service in the 3GPP standard. However, the cell broadcast service exhibits high latency under poor channel conditions. Moreover, the cell broadcast service may be useless for illiterate persons or foreigners since the service just offers text-based messages. For more rapid and reliable delivery, we propose a novel cell broadcast method for 5G wireless emergency alerts. The new technique enables image-based emergency alerts. For the image-based alerts, the presented approach embeds an image code in the alert message. For the image-code embedment, the method effectively exploits the feature of the message structure. The novel approach also offers a cell clustering technique. 5G mobile terminals can rely on the cell clustering in order to achieve a cell diversity, which considerably enhances latency and reliability performance. The experimental results exhibit that the proposed alert method is superior to the conventional technique in terms of latency and reliability.

**INDEX TERMS** Wireless emergency alerts, cell broadcast service, image code, cell clustering, 5G cellular systems.

## I. INTRODUCTION

Much attention has been paid to emergency alert systems, which sustain life qualities in emergency situations [1]. For efficient delivery of emergency alerts, various alert delivery systems have been merged into an aggregated system including integrated public alert and warning system (IPAWS) [2], [3]. In order to deliver emergency alerts rapidly and reliably, modern emergency alert systems exploit advanced information and communications technologies (ICT) including cellular systems and broadcast systems [4]. Especially, cellular systems offer a cell broadcast technology in order to simultaneously deliver emergency alerts to all users in specific cells. The cell broadcast mechanism is called cell broadcast service (CBS) in the third-generation partnership project (3GPP) standard group [5]. Currently, the 3GPP specifies the CBS protocols

for 2G/3G/4G/5G cellular systems [6]. If an alerting authority such as central government specifies an emergency area, cellular networks determine the cells encompassing the area. Then, the base stations broadcast the alert messages to all users in the cells using the CBS protocol. Therefore, the CBS belongs to a location-aware broadcast category [7], [8]. This is a distinct merit over the other alert delivery systems. Furthermore, the CBS allows a rapid delivery due to the simultaneous transmission. However, the conventional CBS exhibits two weak points: text-based message and latency. The CBS just delivers text-based messages for emergency alerts. Usually, text information is less intuitive than image or multimedia information especially in urgent cases. Furthermore, the conventional CBS is unavailable for illiterate persons or foreigners since the CBS just offers text-based messages. In addition to the text limitation, the conventional CBS relies on a repeated delivery, which is used for rebroadcasts in the cases that some users fail in receiving the emergency alert message. The repeated delivery is called

The associate editor coordinating the review of this manuscript and approving it for publication was Hongwei Du.

carousel in the 3GPP [9]. The carousel mechanism causes the conventional CBS to exhibit high latency especially under poor channel conditions. Such latency often frustrates the rapid delivery of emergency alerts. In USA, the public alert system based on the CBS is called wireless emergency alerts (WEA) [10], [11]. Therefore, the WEA system also exhibits the same weak points including text-based message and latency.

We propose a novel WEA technique in 5G cellular systems [12] in order to overcome the weak points of the conventional WEA [10]. The new method includes image code and cell clustering. The novel WEA enables image-based emergency alerts. The presented WEA embeds the novel image code into the text-based message. The WEA reserves unused bits in the text-based message because of the page structure for 5G CBS, which is specified by the 3GPP [9]. If the image code is embedded into the reserved bits, the embedded image code never sacrifices the maximum number of text characters. Note that the maximum number of text characters is just 360 in the WEA system [13]. For the image-code embedment, the proposed method effectively exploits the feature of the 5G CBS message structure. The delivery of image codes is very useful for illiterate persons and foreigners. Furthermore, the image code contributes to the enhancements of latency performance since the length of image code is much smaller than that of text characters in the alert message. Previously, an image-code technique was proposed for CBS-based emergency alerts [27]. However, this method requires additional bytes due to the image indicator, which reduces the maximum length of available text characters in the CBS message. Moreover, the mobile terminal should read the message text character-by-character until it reaches the image indicator, which may cause critical latency problem in urgent cases.

The novel WEA also exploits the proposed cell clustering. The cell clustering consists of initial clustering and adaptive clustering. Since the base stations usually track the mobile terminals in the cells, they can initially determine the clusters of potential outage terminals, which creates the 1st initial clusters. Then, the base stations associate the potential non-outage terminals to each 1st initial cluster, which creates the 2nd initial clusters. After the base station broadcasts the alert message (which includes image code as well as text), some non-outages are selected in each 2nd initial cluster, which initiates the adaptive clustering. The selected non-outages rebroadcast the image code to the outages in the corresponding adaptive cluster, which offers a cell diversity. The adaptive clustering continues until the number of outages is zero in each cluster. Since the presented cell clustering method relies on the image code and the cell diversity, the approach significantly enhances the latency and the reliability performance. Previously, a cluster scheme was presented for emergency alerts [20]. However, the novel approach exhibits the following advantages over the previous work:

- Above of all, the previous work is not suitable for outdoor environments such as cell environments since

the indoor structure already determines initial clustering policy. Therefore, the previous scheme never supports an initial clustering technique, which is required for cell environments. On the other hand, the presented method supports the initial clustering for cell environments.

- The previous work relies on the pre-determined clusters according to the indoor structure. Therefore, the selected non-outage nodes are not always closest to the corresponding outages nodes. On the other hand, the proposed approach supports the adaptive clustering, which adaptively creates new clusters for outages nodes. Therefore, the selected non-outage nodes are always closest to the corresponding outage nodes.
- The previous work relies on selection combining (SC) technique as a diversity. On the other hand, the proposed work relies on maximal ratio combining (MRC) technique as a diversity. Note that MRC is superior to SC in terms of diversity performance [23].

Experimental evaluation reveals the validity of the proposed WEA approach in 5G cellular systems. The experimental results show that the proposed WEA is superior to the conventional WEA [10] in terms of latency and reliability.

## II. 5G CBS PROTOCOL

Since the conventional WEA adopts the CBS protocol for 5G cellular systems, we describe the 5G CBS protocol [9] as a benchmark in section II.

Like the cases of 2G, 3G, and 4G cellular systems, 5G systems adopt the CBS protocol for emergency alert services. 5G cellular systems are based on highly flexible and scalable networks [12]. 5G systems also offer the services for enhanced mobile broadband (eMBB), ultra-reliable low latency communications (URLLC), and massive machine type communications (mMTC) [12].

Figure 1 illustrates the service-based architecture (SBA) of 5G cellular systems. In Figure 1, the 5G core network (CN) consists of various service functions including access and mobility function (AMF), session management function (SMF), policy control function (PCF), network slice selection function (NSSF), network exposure function (NEF), unified data management (UDM), cell broadcast center function (CBCF), and public warning system/interworking function (PWS-IWF). The service functions are interfaced each other via a service interface [14]. Among those service functions, CBCF and AMF are used for the CBS protocol. In Figure 1, radio access network (RAN) includes base stations. In Figure 1, user equipment (UE) indicates a mobile terminal. Therefore, UE is interfaced to RAN via a wireless channel in Figure 1.

Figure 2 illustrates the network architecture of 5G CBS [9]. The network architecture consists of cell broadcast entity (CBE), CBCF, AMF, RAN, and UE. In Figure 2, the CBE acts as a gateway between network operator and CBCF. Therefore, the CBE receives alert messages from the network operator, and relays the messages to the CBCF. The alert message format is determined by the network operator.

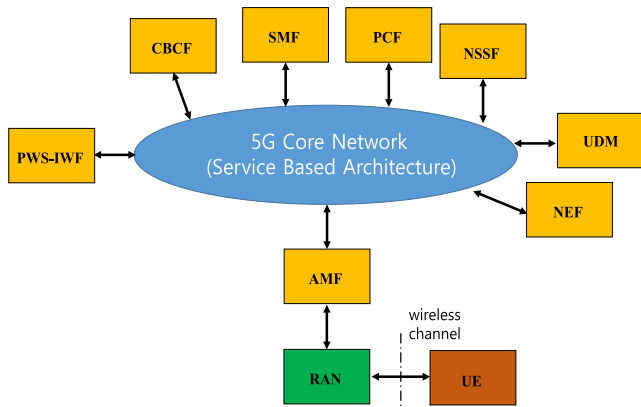


FIGURE 1. The service-based architecture of 5G.

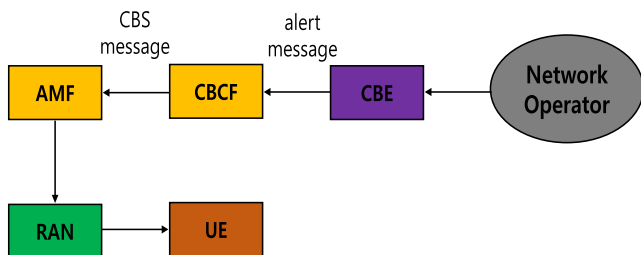


FIGURE 2. The network architecture of 5G CBS.

The CBCF identifies the corresponding AMFs using the emergency area information of the received alert message. Then, the CBCF transforms the alert message format into the CBS message format, which is determined by the 3GPP standard [9]. Finally, the CBCF sends the CBS messages to the identified AMFs.

Figure 3 illustrates the procedure of the CBS message delivery in 5G cellular systems [9]. The procedure is described as follows [9]:

- 1 The CBE sends the original alert messages (from the network operator) to the CBCF using a request message (Emergency Broadcast Request).
- 2 After identifying the related AMFs, the CBCF embeds the original alert message and several delivery attributes into the 3GPP CBS message (Write-Replace Warning Request). The 3GPP standard [9] specifies the format of the 3GPP CBS message. Then, the CBCF sends the 3GPP CBS message to the identified AMFs.
- 3 Each AMF sends back the 3GPP confirm message (Write-Replace Warning Confirm) to the CBCF, which indicates that the AMF has started the distribution of the 3GPP CBS message to the RAN nodes.
- 4 The CBCF sends back a response message (Emergency Broadcast Response) to the CBE if it receives the 3GPP confirm message from the AMF.
- 5 Using the delivery attributes, each AMF identifies the RAN nodes corresponding to the emergency area. Then, the AMF forwards the 3GPP CBS message to the identified RAN nodes.

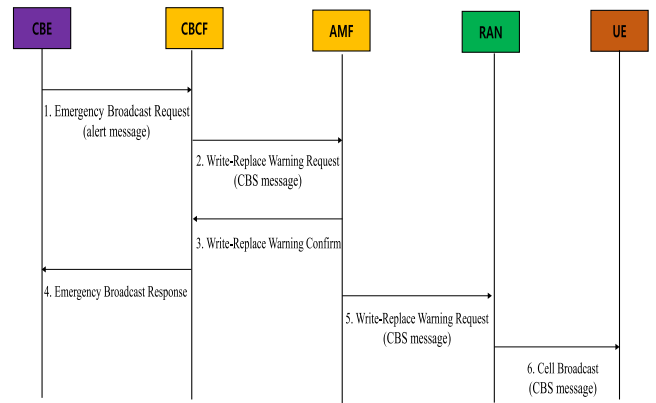


FIGURE 3. The procedure of the CBS emergency message delivery in 5G cellular systems.

- 6 Using the delivery attributes, each RAN identifies the cells corresponding to the emergency area. Then, the base station broadcasts the CBS message to all users in each identified cell.

Figure 4 illustrates the CBS message broadcast in the identified cell. In the cell, all users receive the CBS alert message from the base station. As shown in Figure 4, the identified cell encompasses the emergency area. Therefore, alerting authorities can effectively deliver emergency alert message to the persons, who are located in the emergency area. In Figures 3 and 4, the CBS message is broadcast to end users via a wireless channel. The 3GPP specification [15] specifies a radio protocol for the broadcast. Figure 5 illustrates the 5G radio protocol for CBS. For the wireless broadcast, the CBS message is embedded into the system information block (SIB) 8 [15]. In Figure 5, the radio resource control (RRC) is responsible for the broadcast of the SIB 8 to all mobile terminals in a cell. The RRC belongs to layer 3. As shown in Figure 5, the SIB 8 successively descends into packet data convergence protocol (PDCP), radio link control (RLC), and medium access control (MAC) sublayers, which belong to layer 2. For the transfer of the SIB 8 from RLC to MAC, broadcast control channel (BCCH) is used, which

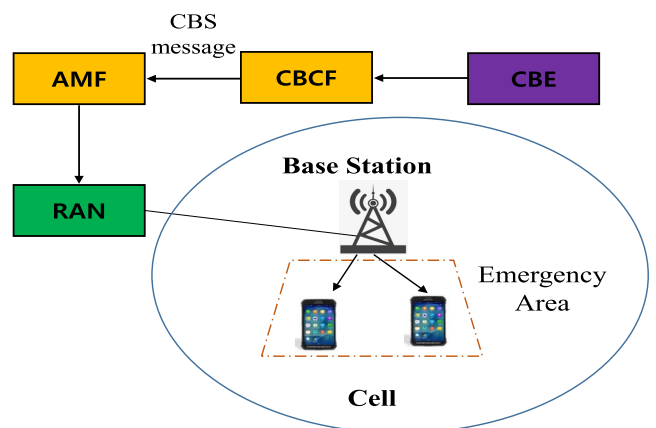


FIGURE 4. The CBS message broadcast in the identified cell.

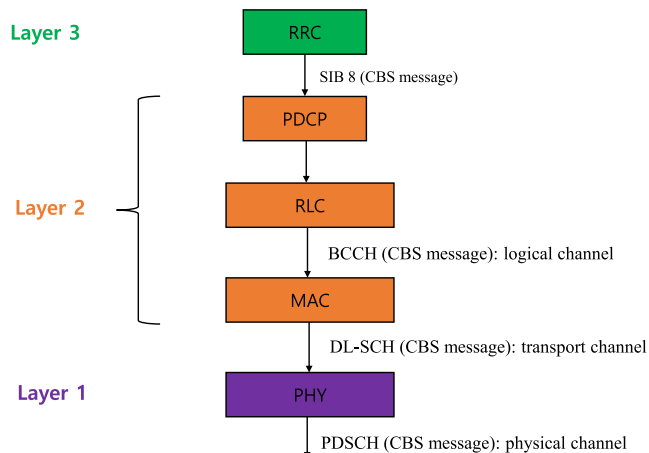


FIGURE 5. The 5G radio protocol for CBS.

belongs to logical channel. For the transfer of the SIB 8 from MAC to physical (PHY) layer (layer 1), downlink shared channel (DL-SCH) is used, which belongs to transport channel. Finally, the SIB 8 is broadcast to all mobile terminals in a cell via physical downlink shared channel (PDSCH), which belongs to physical channel.

Figure 6 shows the data structure of SIB 8 [15]. The CBS text message is embedded into the warningMessageSegment in Figure 6. The other elements (message identifier, serial number, segment type, segment number, and so on) denote the parameters for the CBS message in Figure 6. In 5G systems, the SIB’s include small-sized data for the control of mobile terminals in a cell. Therefore, the conventional WEA just delivers text-based messages. As stated earlier, the text-based messages are unavailable for illiterate persons or foreigners. In addition, the 5G CBS just relies on the carousel method for rebroadcasts [9]. However, the mobile terminals at the cell edge likely fail in decoding the CBS message even after the carousel method. This leads to low reliability and high latency in the conventional WEA system.

```

SystemInformationBlockType8::SEQUENCE {
    messageIdentifier          BIT STRING (SIZE (16)),
    serialNumber               BIT STRING (SIZE (16)),
    warningMessageSegmentType  ENUMERATED {notLastSegment, LastSegment},
    warningMessageSegmentNumber INTEGER (0 ... 63),
    warningMessageSegment      OCTET STRING,
    dataCodingScheme           OCTET STRING (SIZE (1)) OPTIONAL,
    warningAreaCoordinateSegment OCTET STRING OPTIONAL,
    lateNonCriticalExtension    OCTET STRING OPTIONAL,
    ...
}
    
```

FIGURE 6. The data structure of SIB 8.

### III. THE NOVEL WEA APPROACH

The novel WEA approach includes the proposed image-based alert and cell clustering techniques.

#### A. IMAGE-BASED METHOD

Like the conventional WEA [10], the proposed method assumes the GSM-7 coded text message [16]. Note that most

European languages including English are encoded using the GSM-7. It is also assumed that all necessary image symbols are pre-stored in mobile terminals.

Table 1 shows the structure of the CBS message for 5G cellular systems [9]. As indicated in Table 1, the CBS message consists of pages, and each page has 82-octet size [9]. In each page information of Table 1, the maximum number of characters ( $max\_char$ ) can be calculated as follows:

$$max\_char = \left\lfloor \frac{82 \times 8}{m} \right\rfloor, \tag{1}$$

TABLE 1. The Structure of CBS Message for 5G.

Octets	Description
1	Number of pages ( $N$ )
82	Page information 1
1	Page length 1
82	Page information 2
1	Page length 2
⋮	⋮
⋮	⋮
82	Page information $N$
1	Page length $N$

where  $m = 7$  according to the GSM-7 code [16], and  $\lfloor x \rfloor = n$  ( $n$  is an integer and  $x - 1 < n \leq x$ ). Using (1), the minimum number ( $l$ ) of reserved bits for zero padding can be calculated in each page information as follows:

$$l = 82 \times 8 - max\_char. \tag{2}$$

Using (1) and (2), the last 5 bits are always reserved for zero padding in each page [13].

Using the feature of the CBS message structure (Table 1), we can effectively set up a novel image code in the proposed WEA approach. Figure 7 illustrates the 5-bit image code, which is embedded in the last 5 bits of the message page. In the page information of Table 1, the last 5 bits (reserved for zero padding) can be used for the 5-bit image code. The image

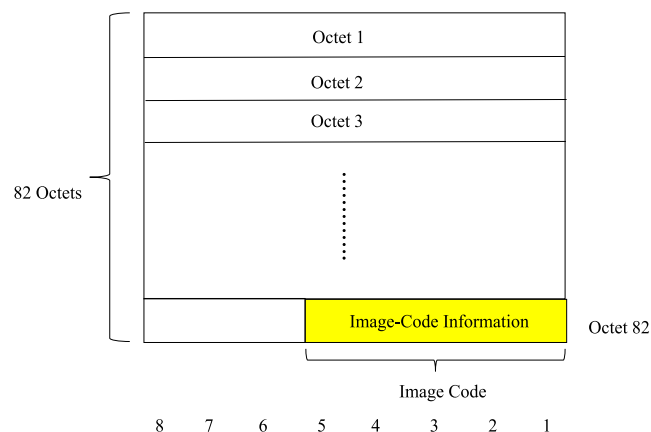


FIGURE 7. The image code embedded in the last 5 bits of the message page.

code represents an image symbol to be displayed in mobile terminals. Since 5 bits are used for the image code, 32 image symbols can be pre-stored in mobile terminals. Note that the use of the image code never sacrifices the maximum length of text characters since the 5-bit image code is embedded into the reserved bits (for zero padding). Figure 8 illustrates the procedure of mobile terminal for the image-based alert method. If the mobile terminal receives the CBS message, it determines the cyclic redundancy check (CRC) for the decoding state (success or failure). Note that the MAC of Figure 5 performs the CRC detection for the CBS message. If the decoding state of the received CBS message is success, the mobile terminal displays the image symbol (corresponding to the image code) in addition to the text message. If the CRC fails, the mobile terminal does not display any image symbol as well as the text message.

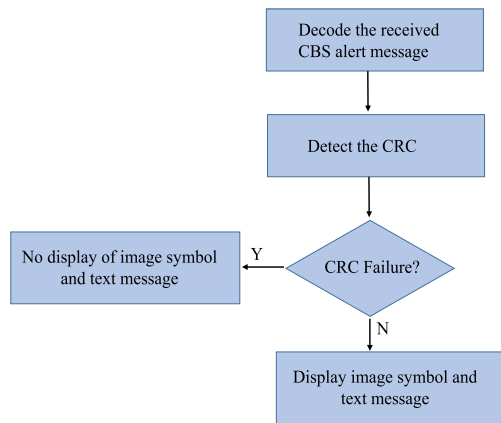


FIGURE 8. The procedure of mobile terminal for the image-based alert method.

Figure 9 illustrates the example of an image symbol, which can be used for the image-based emergency alert method. This symbol includes Spanish texts as well as English texts, which represents an emergency type (earthquake in Figure 9). Therefore, Spanish-speaking foreigners can easily recognize the emergency type even in the case that main text is written in English in the alert message. Any other language can be displayed in the same way.

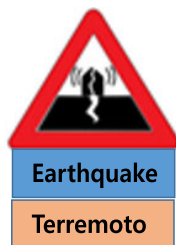


FIGURE 9. The example of an image symbol (earthquake) for the image-based alert method.

Figure 10 illustrates the example of the image and text display in the case of image-based alert method. When an

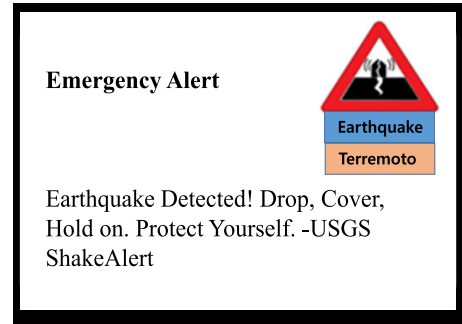


FIGURE 10. The example of the image and text display in the case of image-based alert method.

emergency such as earthquake occurs, the mobile terminals receive the CBS message in an emergency area. If the CRC success is detected, the terminals can use the image code for the display, which is embedded in the last 5 bits of the message page. Therefore, the mobile terminals display the corresponding image symbol as well as the text, which is shown in Figure 10.

**B. CELL CLUSTERING TECHNIQUE**

The cell clustering approach consists of initial clustering and adaptive clustering. Figure 11 illustrates the procedure of the proposed cell clustering. Since the base station can track the mobile terminals in the corresponding cell, it performs the initial clustering and the adaptive clustering. The base station relies on the K-means algorithm [17] in order to determine the initial clusters. Then, the base station performs the adaptive clustering using outage and non-outage terminals. It continues the adaptive clustering until the number of outage terminals is zero in the cell. Therefore, the cell clustering of Figure 11 may require a high computation. In order to handle the high computation of the cell clustering, the base

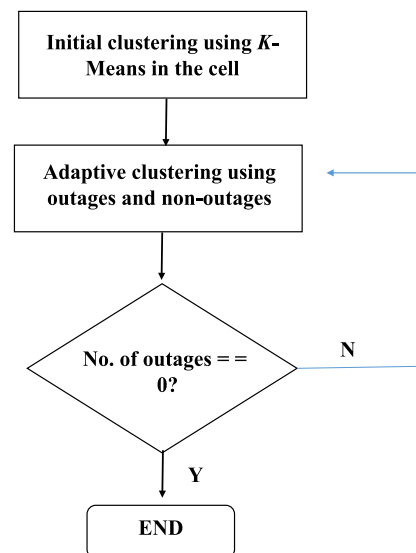


FIGURE 11. The procedure of the proposed cell clustering technique.

station can rely on a multi-access edge computing (MEC) server, which is usually used for high computation in 5G cellular systems [18].

The initial clustering consists of outage sub-region, 1st initial clusters, and 2nd initial clusters. Figure 12 illustrates the outage sub-region for the initial clustering. Since the mobile terminals at the cell edge are most likely to fail in decoding the CBS message, the base station determines the outage sub-region around the cell edge for the initial clustering as shown in Figure 12. Then, the base station (or MEC) uses the  $K$ -means algorithm [17] to achieve the 1st initial clusters in the outage sub-region of the cell, which is illustrated in Figure 13. The 1st initial clusters include potential outage terminals.

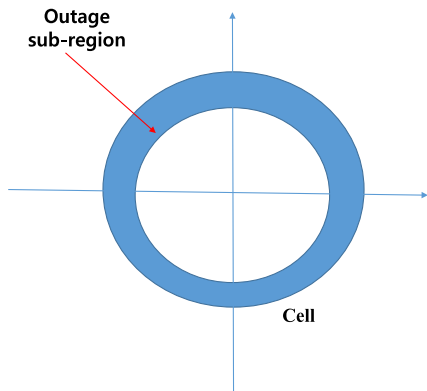


FIGURE 12. The outage sub-region of the cell for the initial clustering.

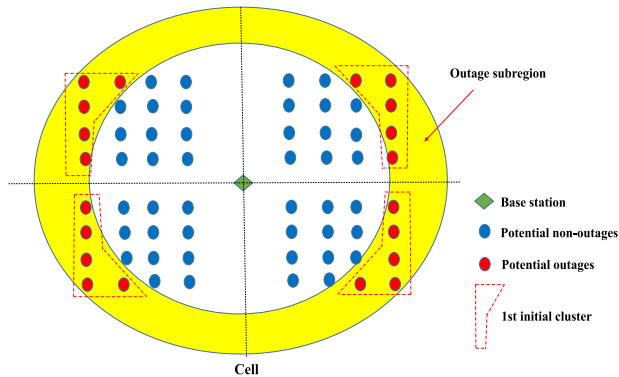


FIGURE 13. The 1st initial clusters in the outage sub-region of the cell.

Finally, the base station (or MEC) associates the potential non-outage terminals to each corresponding 1st initial cluster, which creates the 2nd initial cluster. Figure 14 illustrates the generated 2nd initial clusters using the association.

Figure 15 depicts the procedure of the association for the creation of the 2nd initial clusters in the initial clustering. In the association procedure, the base station (or MEC) finds the average location of the potential outages in each 1st initial cluster. Then, it determines the  $M$  potential non-outage terminals in the area outside the outage sub-region of the cell. The locations of the selected potential

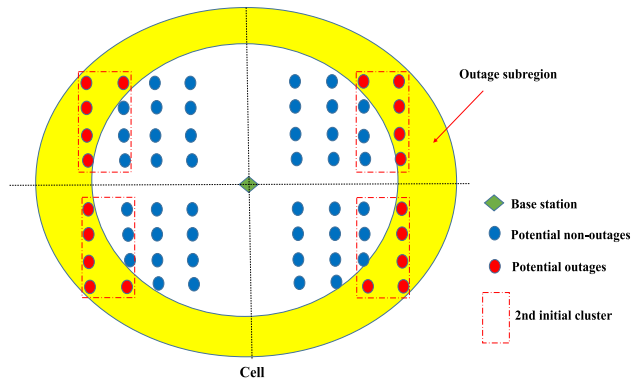


FIGURE 14. The 2nd initial clusters in the cell.

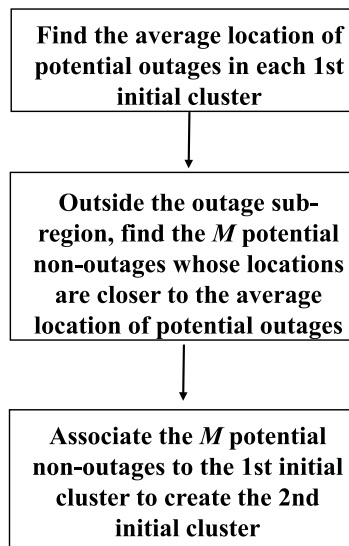


FIGURE 15. The association procedure for the creation of the 2nd initial clusters.

non-outages are closer to the average location of the potential outages in the corresponding 1st initial cluster. Finally, the base station (or MEC) associates the selected potential non-outages to the 1st initial cluster, which creates the corresponding 2nd initial cluster.

After the initial clustering, the base station continues the tracking of the mobile terminals in the cell. According to the varying locations of the terminals, the base station (or MEC) can change the terminal members in the initial clusters. In addition, the base station (or MEC) can change the potential states (outage or non-outage) of the terminals in the initial clusters. If an emergency occurs, the base station broadcasts the CBS message (which includes image code as well as text) to the mobile terminals in the cell according to the CBS protocol [15]. In this case, the base station (or MEC) still maintains the 2nd initial clusters. As soon as the mobile terminals receive the CBS message, they can be classified into true non-outage nodes and true outage nodes according to the success or failure of message decoding, respectively. Then,  $L$  ( $L \leq M$ ) true non-outages are selected in each 2nd initial cluster. The locations of the selected non-outages are closer

to the average location of the true outages in each 2nd initial cluster. Using the selected non-outages and the true outages, each 2nd initial cluster is re-clustered into a corresponding adaptive cluster. Figure 16 illustrates the created adaptive clusters. In each adaptive cluster, the selected non-outages rebroadcast the image code (in the received CBS message) to the true outages using the proposed diversity approach.

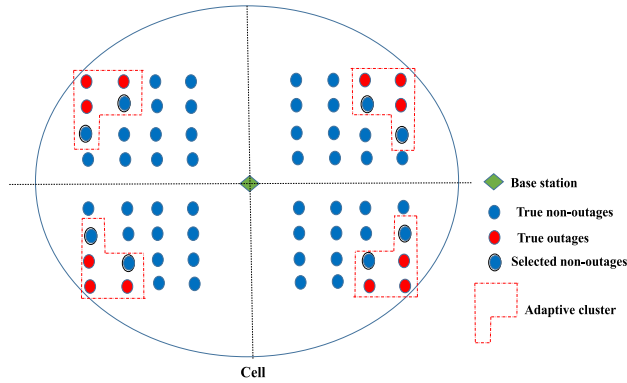


FIGURE 16. The illustration of the adaptive clusters.

When the outage terminals receive the image code in an adaptive cluster, some outage nodes can be changed into non-outage nodes if the decoding is successful. Therefore, the adaptive cluster needs to be changed into a new adaptive cluster. Figure 17 depicts the procedure of the adaptive clustering. The base station (or MEC) re-clusters the latest outages in each previous adaptive cluster. Then, it finds the average location of the latest outages in each re-cluster. Then, it finds the  $L$  non-outages whose locations are closer to the average location of the outages each re-cluster. Finally, it adds the  $L$  non-outages to the corresponding re-cluster, which produces a new adaptive cluster. After the new adaptive cluster is created, the selected non-outages rebroadcast the image code to the outages (in each new cluster) using the proposed diversity technique. As depicted in Figure 11, the base station (or MEC) continues the adaptive clustering until the number of outage terminals is zero in the cell.

The proposed cell clustering enhances the latency and the reliability performance as follows:

- In each adaptive cluster, the non-outages just rebroadcast the image code. When the outages successfully decode the received image code, the outage users (including foreigners) can easily recognize the emergency type using the image symbol, which can be displayed on the terminal screen as shown in Figure 18. Therefore, they can quickly react to the recognized emergency. Furthermore, the length (5 bits) of the image code is much shorter than that of text as indicated in Figure 7. The shorter length leads to better latency performance, which will be verified in section III-D.
- In each adaptive cluster, the selected non-outages are closer to the average location of outages. In average, the distance between the outages and the selected

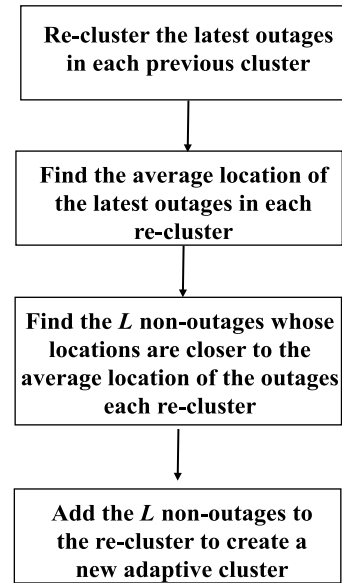


FIGURE 17. The procedure of the adaptive clustering.

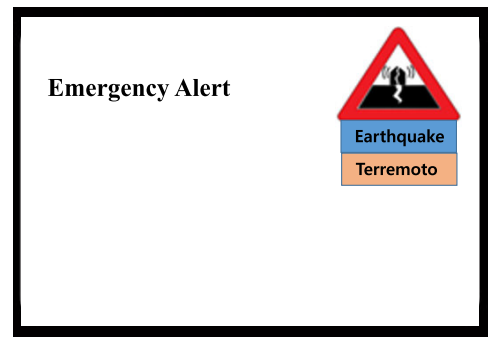


FIGURE 18. The example of the image symbol display on terminal screen.

non-outages is shortest. The simplified path-loss model describes the relation between transmitted signal power and received signal power [19]. The numerical expression for the simplified path-loss model is given as follows:

$$P_r = P_t K \left( \frac{d_0}{d} \right)^\gamma, \quad (3)$$

where  $P_t$  and  $P_r$  denote the transmitted signal power and the received signal power, respectively. In (3),  $K$ ,  $d_0$ ,  $\gamma$ , and  $d$  are a unit-less constant, a reference distance, a path-loss component, and a distance between transmitter and receiver, respectively. Therefore, shorter distance ( $d$ ) guarantees larger received power ( $P_r$ ) in (3). This indicates that the outages can relatively receive larger signal power from the selected non-outages. The larger received signal power usually leads to better reliability performance [20].

- In each adaptive cluster, the selected non-outages rebroadcast the image code using the proposed diversity approach, which is described in section III-C. Note that

most diversity techniques usually enhance reliability performance [19].

**C. CELL DIVERSITY**

For the proposed cell diversity approach, we assume the following features of 5G cellular systems [12]:

- Device-to-device communications
- Mobile terminals employing IoT devices, which include IEEE 802.11 protocols based on orthogonal frequency division multiplexing (OFDM) [21]

Therefore, the selected non-outage mobile terminals rely on the OFDM-based IEEE 802.11 protocols [22] for the rebroadcasts of the image code in the adaptive clustering. Note that the OFDM-based IEEE 802.11 protocols use a beacon frame in order to broadcast a buffered information including the image code [22].

Figure 19 illustrates the allocation of image-code for the selected non-outages in each adaptive cluster. In order to avoid the interferences from the other selected non-outages in the cluster, each selected non-outage adopts the allocation policy of Figure 19. Since the non-outages rely on the OFDM technique for the rebroadcasts of the image code, they can allocate the image-code information to the specified subcarrier sub-band in the OFDM block as shown in Figure 19. Therefore, the non-outages can rebroadcast the packets without any interference in each cluster. If the  $i$ th non-outage produces one OFDM block including the image-code information in the cluster, the information symbol at the  $k$ th subcarrier in the OFDM block is denoted as  $X[k]$ , and is expressed as follows:

$$X[k + J(i - 1)] = x_i[k], \tag{4}$$

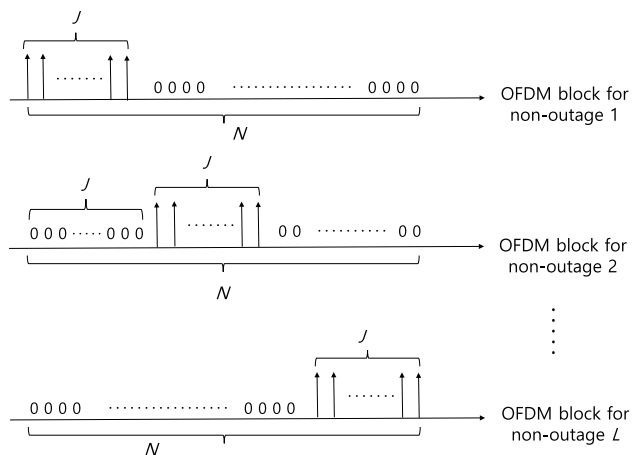


**FIGURE 19.** The allocation of image-code information for the selected non-outages in each adaptive cluster.

where  $x_i[k]$  denotes the image-code symbol at the  $k$ th subcarrier for the  $i$ th selected non-outage in the cluster. In (4),  $i = 1, 2, \dots, L$ , and  $k = 0, 1, \dots, J - 1$ , where  $L$  and  $J$  denote the number of the selected non-outages in the cluster and the length of the subcarriers for the image-code information,

respectively. In (4),  $J$  is defined as follows:

$$J = \frac{N}{L}, \tag{5}$$

where  $N$  denotes the number of the subcarriers in one OFDM block. Using the OFDM protocol including cyclic prefix [21], the outages of the cluster receive the following information symbol:

$$Y_i[k] = X[k + J \cdot (i - 1)] \sum_{l=1}^P h^{(l)}[k + J \cdot (i - 1)] + Z[k + J \cdot (i - 1)], \tag{6}$$

where  $i = 1, 2, \dots, L$  and  $k = 0, 1, \dots, J - 1$ , and  $P$  denotes the number of clusters in the cell. In (6),  $h^{(l)}[k + J \cdot (i - 1)]$  and  $Z[k + J \cdot (i - 1)]$  denote the channel parameter between the  $i$ th selected non-outage and the outage in the  $l$ th cluster, and the additive white Gaussian noise (AWGN), respectively at the  $k$ th subcarrier. In order to achieve a diversity, the outages of the cluster calculate the metric  $Y[k]$  as follows:

$$Y[k] = \sum_{i=1}^L H_i^*[k] Y_i[k], \tag{7}$$

where  $k = 0, 1, \dots, J - 1$ , and  $*$  denotes the complex conjugate operator. In (7),  $H_i[k]$  is defined as follows:

$$H_i[k] = \sum_{l=1}^P h^{(l)}[k + J \cdot (i - 1)]. \tag{8}$$

Finally, the outages decode the metric of (7) and extract the image code. This indicates that the proposed diversity approach is equivalent to the maximal ratio combining (MRC) diversity technique [23], which will be verified in section IV. Since the MRC diversity method guarantees the optimal performance [23], the presented cell diversity significantly improves reliability performance.

**D. PERFORMANCE ANALYSIS**

As stated earlier, the proposed image-code technique enhances the latency performance. For the analysis of latency performance, we assume a random variable  $\eta_i$ , which denotes the number of total broadcasts for successful transmission of a CBS alert message to the  $i$ th mobile terminal in a cell. Thus, the expected value of  $\eta_i$  is expressed as follows [24]:

$$E[\eta_i] = \sum_{k=0}^{\infty} (k + 1) \Pr_i(K = k), \tag{9}$$

where  $K$  denotes the number of attempts required to successfully transmit the CBS alert message. In (9),  $\Pr_i(K = k)$  defines the probability that the first  $k$  attempts will fail and the  $(k + 1)$ th attempt will succeed for the  $i$ th mobile terminal. Since  $K$  follows a geometric distribution in (9),  $\Pr_i(K = k)$  can be expressed as follows [20]:

$$\Pr_i(K = k) = p_{e,i}^k (1 - p_{e,i}), \tag{10}$$



where  $p_{e,i}$  denotes the probability of an erroneous transmission of the CBS alert message to the  $i$ th mobile terminal. After the substitution of (10) into (9),  $E[\eta_i]$  of (9) can also be expressed as follows:

$$E[\eta_i] = \frac{1}{1 - p_{e,i}}. \quad (11)$$

In the cell, the CBS alert message is independently broadcast to all mobile terminals. If a random variable  $\eta$  is defined as the number of total broadcasts for successful transmission of a CBS alert message to  $Q$  mobile terminals in the cell, the expected value of  $\eta$  can be expressed as follows:

$$E[\eta] = E[\eta_1]E[\eta_2] \cdots E[\eta_Q] \\ = \frac{1}{(1 - p_{e,1})(1 - p_{e,2}) \cdots (1 - p_{e,Q})}. \quad (12)$$

In order to lessen the number of rebroadcasts, we need to diminish the value of  $E[\eta]$ . In (12), we have to decrease  $p_{e,i}$  in order to reduce  $E[\eta]$ . In (12),  $p_{e,i}$  can be expressed as follows:

$$p_{e,i} = 1 - (1 - p_{b,i})^l, \quad (13)$$

where  $p_{b,i}$  denotes the bit error rate (BER) of the CBS alert message to the  $i$ th mobile terminal. In (13),  $l$  denotes the message size. Since  $1 - p_{b,i}$  is less than 1, smaller  $l$  leads to smaller  $p_{e,i}$ . Note that the size (5 bits) of the image-code is much less than that of the text message in the CBS message. Therefore, it is much more possible to decode the image code successfully. This considerably reduces the number of rebroadcasts, which in turn leads to much smaller latency.

Furthermore, the proposed cell diversity enhances the reliability performance. Since the presented diversity method is equivalent to the MRC technique as stated earlier, we consider the theoretical BER performance ( $P_b$ ) for the MRC diversity [25] as follows:

$$P_b = \frac{1}{2^L} \left( 1 - \sqrt{\frac{1}{1 + \left(\frac{E_b}{N_0}\right)^{-1}}} \right)^L \\ \times \sum_{l=0}^{L-1} \binom{L-1+l}{l} \frac{1}{2^l} \left( 1 + \sqrt{\frac{1}{1 + \left(\frac{E_b}{N_0}\right)^{-1}}} \right)^l, \quad (14)$$

where  $L$  denotes the number of the selected non-outages in the cluster. In (14), larger  $L$  leads to smaller BER ( $P_b$ ). Since  $L > 1$  in (14), the proposed cell diversity guarantees better reliability performance.

#### IV. EXPERIMENTAL EVALUATION

The experimental evaluation exhibits the effectiveness of the proposed 5G wireless emergency alerts based on image code and cell clustering.

Table 2 summarizes the experimental parameters. The carrier frequency of 5G systems is 3.5 GHz. As the fading channel model for 5G, Jakarta channel model [26] is adopted in this evaluation. In the channel model, each path follows

TABLE 2. The experimental parameters.

Parameter	Value/Property
Carrier frequency of 5G systems	3.5 GHz
Fading channel	Jakarta
Cell radius	1 Km
Number of mobile terminals per cell	200
Distribution of mobile terminals	Uniform
Transmit power of base station	1 W
Transmit power of mobile terminal for rebroadcast	0.5 mW
Number of the subcarriers in one OFDM block for rebroadcast ( $N$ )	64
Number of the selected non-outage terminals for the diversity in each cluster ( $L$ )	4

Rayleigh distribution [19]. In this experiment, the cell radius for 5G is assumed to be 1 Km. In each cell, the number of mobile terminals is set to 200. In each cell, it is assumed that the mobile terminals are uniformly distributed. For the broadcast of the CBS alert message, it is also assumed that the transmit power of the base station is 1 W in this evaluation. For the rebroadcasts of the image code, the transmit power of the mobile terminal is set to be 0.5 mW. Table 2 indicates that  $N$  and  $L$  are set to 64 and 4, respectively in (5). Therefore,  $J$  is set to 16 in (5).

The proposed approach uses the image-code information for the rebroadcast. Figure 20 exhibits a comparison of the latency performance for the proposed image-code transmission and the conventional text-message transmission in the CBS message alert. In order to better investigate the effect of the length on the latency performance, we did not include the cell clustering and the cell diversity techniques in the performance evaluation. As shown in Figure 20, the latency of the proposed image code is much lower than that of the conventional text message over the entire range of  $E_b/N_0$ . Figure 20 reveals that the proposed image-code transmission

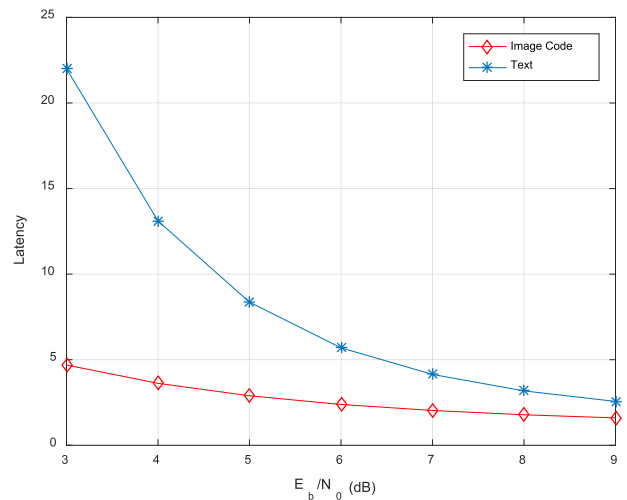
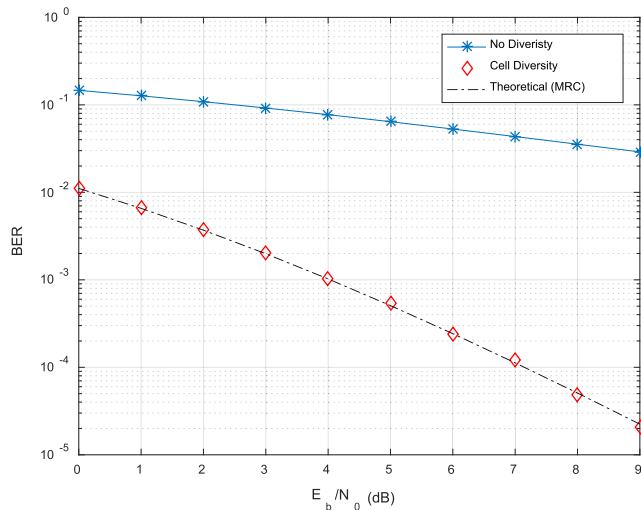


FIGURE 20. The comparison of the latency performance for the proposed image-code transmission and the conventional text-message transmission.

is much superior to the conventional text-message transmission in terms of latency. This is due to the fact that the length of the image code is much shorter than that of the text message. As indicated in (11) to (13), shorter length leads to better latency performance, which was verified in Figure 20. Therefore, the mobile terminals just transmit the image-code information instead of the full text information in order to achieve better latency performance as stated earlier.

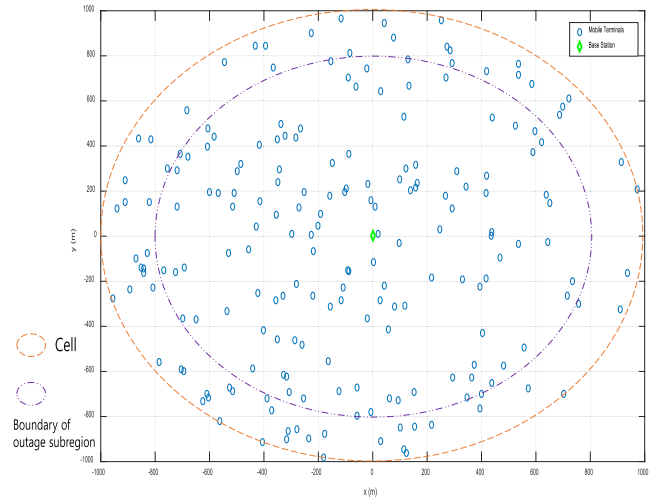
Figure 21 exhibits a comparison of BER performance for the proposed diversity case (cell diversity) and the diversity-free case (no diversity). As shown in Figure 21, the proposed cell diversity considerably enhances the BER performance, which leads to better reliability performance. Figure 21 also shows that the BER performance of the cell diversity is identical to the theoretical BER performance of the MRC technique, which is given in (14). This confirms that the presented cell diversity effectively exploits the diversity of the MRC approach.



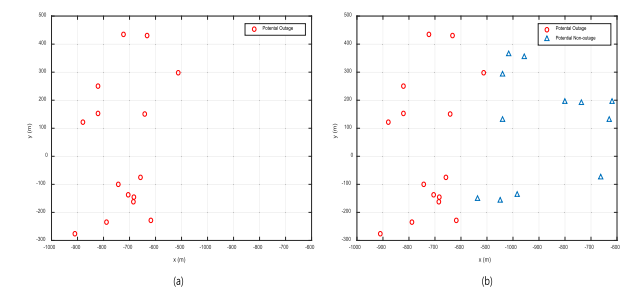
**FIGURE 21.** The comparison of the bit error rate (BER) performance for the proposed diversity case (cell diversity) and the diversity-free case (no diversity).

Figure 22 illustrates the placements of mobile terminals in a cell for the experimental evaluation. Figure 22 shows that the 200 mobile terminals are randomly placed in the cell. In Figure 22, the mobile terminals outside the boundary of outage subregion belong to the outage subregion. The mobile terminals are used as the potential outages for the 1st initial clusters in the initial clustering, which are illustrated in Figure 13. The *K*-means algorithm [17] uses the potential non-outages to produce the 1st initial clusters. Figure 22 also shows that the base station is located at the center (0,0) of the cell. The base station broadcasts the CBS alert message to the mobile terminals in the cell.

Figure 23 illustrates the placements of potential outages and non-outages in the initial clustering. The initial clustering generates the 1st initial and the 2nd initial clusters. Figure 23(a) shows the placements of potential outages in the 1st initial cluster, which is achieved using the



**FIGURE 22.** The placements of mobile terminals in a cell.



**FIGURE 23.** The placements of potential outages and non-outages in the initial clustering.

*K*-means algorithm. In Figure 23(a), the potential outages belong to the outage subregion of Figure 22. The base station creates the 2nd initial clusters based on the 1st initial clusters. Figure 23(b) shows the placements of potential outages and non-outages in the 2nd cluster, which is based on the 1st cluster of Figure 23(a). As depicted in Figure 15, the base station associates the potential non-outages to the 1st initial cluster of Figure 23(a), which generates the corresponding 2nd initial cluster of Figure 23(b). In Figure 23(b), the number of potential non-outages is  $3L$ , where  $L$  is 4 in Table 2. Note that the associated non-outages are closer to the average location of the potential outages as stated in Figure 15. After the base station sets up the 2nd initial clusters, it is ready to broadcast the CBS alert message.

Figure 24 illustrates the placements of true outages and non-outages in the adaptive clustering. Figure 24(a) shows true outages and non-outages in the 2nd initial cluster of Figure 23(b) after the base station broadcasts the CBS alert message. There are 17 true outages in Figure 24(a). Among the 10 true non-outages in Figure 24(a), the base station selects the 4 non-outages for the cell diversity, and creates the 1st adaptive cluster, which consists of the 4 selected non-outages and the 17 true outages. Then, the 4 selected

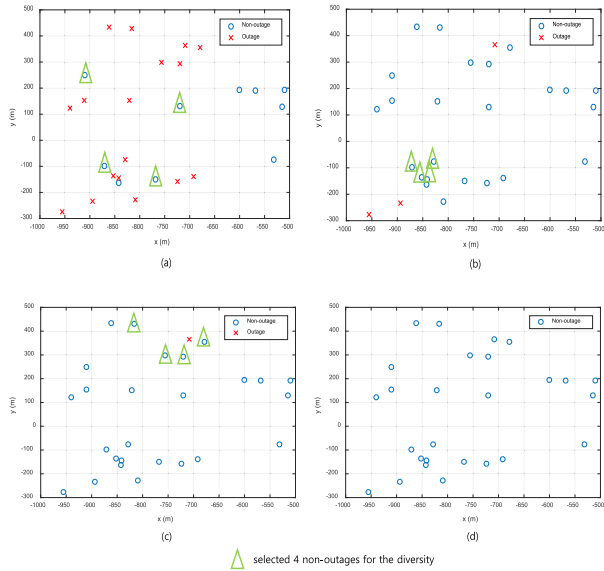
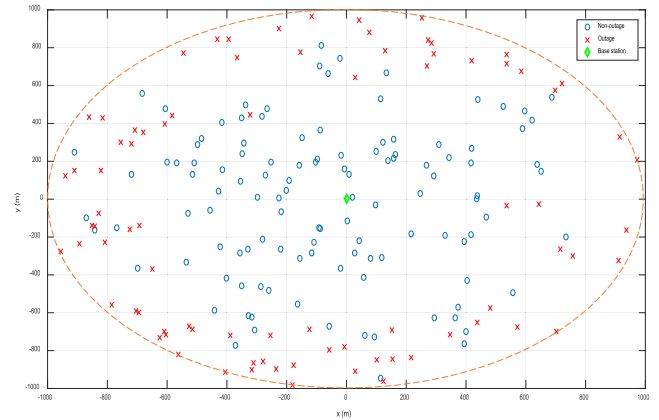


**FIGURE 24.** The placements of true outages and non-outages in the adaptive clustering.

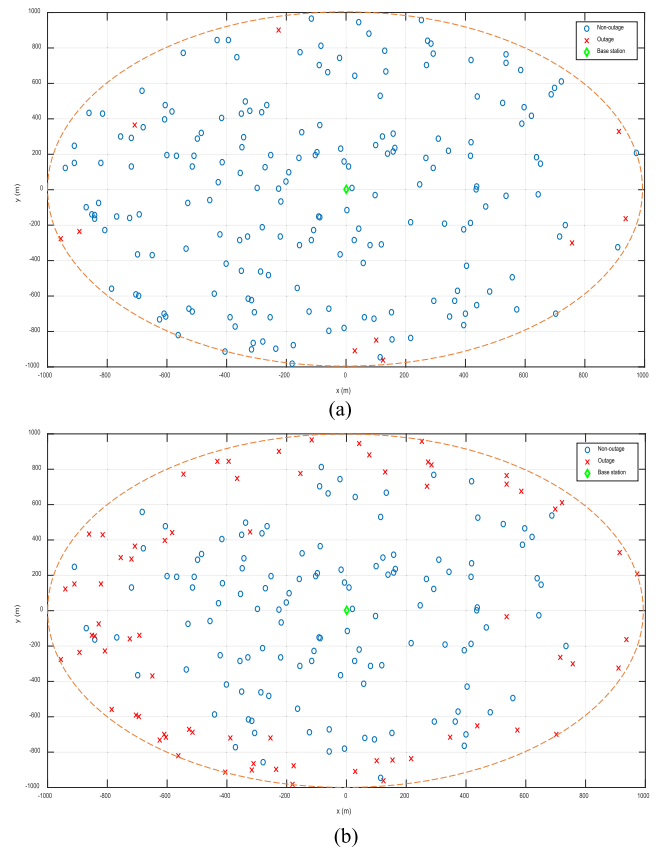
non-outages rebroadcast the image-code information using the cell diversity. Figure 24(b) shows true outages and non-outages after the 1st rebroadcast. There are 3 true outages. Among the 24 true non-outages, the base station selects the 4 non-outages of Figure 24(b) for the cell diversity, and creates the 2nd adaptive cluster, which consists of the 4 selected non-outages and the 3 true outages. Then, the 4 selected non-outages rebroadcast the image-code information using the cell diversity. Figure 24(c) shows true outage and non-outages after the 2nd rebroadcast. There is still one true outage. Among the 26 true non-outages, the base station selects the 4 non-outages of Figure 24(c) for the cell diversity, and creates the 3rd adaptive cluster, which consists of the 4 selected non-outages and the 1 true outage. Then, the 4 selected non-outages rebroadcast the image-code information using the cell diversity. Figure 24(d) shows true non-outages after the 3rd rebroadcast. Finally, there is no more outage. Therefore, the base station finishes the adaptive clustering procedure.

Figure 25 exhibits the distribution of outages and non-outages after the broadcast of the base station. In the cell, the distribution of the mobile terminals follows that of Figure 22. In Figure 25, the base station broadcasts the CBS alert message, which consists of full text message and image-code. After the broadcast, 83 mobile terminals fail in decoding the CBS message successfully in the cell. Therefore, the success rate is just 58.5%. This indicates that more than 40% of the users have no information even in a serious emergency case. Therefore, a rebroadcast mechanism is required for reliable alert delivery.

Figure 26 exhibits the comparison of the outage and the non-outage distributions for the proposed approach and the conventional method after the 1st rebroadcast. The proposed WEA approach relies on the image-code delivery, the cell

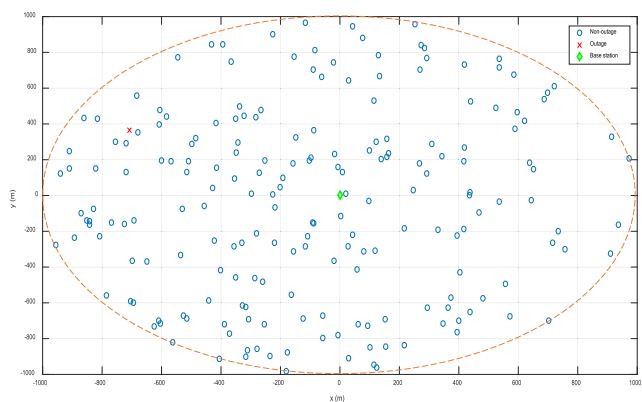


**FIGURE 25.** The distribution of outages and non-outages after the broadcast of the base station.

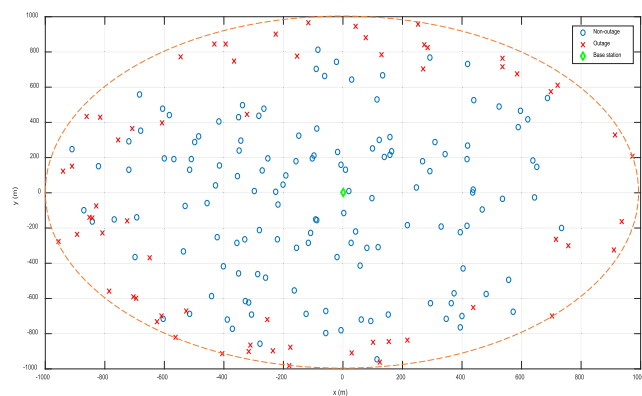


**FIGURE 26.** The comparison of the outage and the non-outage distributions for the proposed approach and the conventional method after the 1st rebroadcast.

clustering, and the cell diversity for the rebroadcast. The conventional WEA method relies on the carousel technique [9, 20] for the rebroadcast. Unlike the novel rebroadcast mechanism, the carousel technique just use the same base station for the rebroadcast. Therefore, it is more likely that the mobile terminals at the cell edge still fail in decoding the alert message especially under poor channel conditions. Figure 26(a) shows the outage and the non-outage distributions for the proposed method after the 1st rebroadcast.



(a)

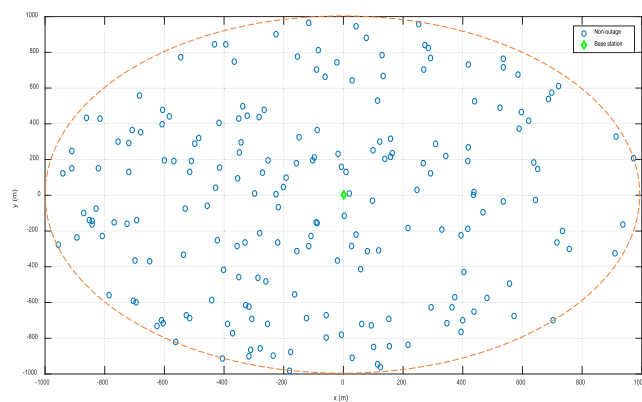


(b)

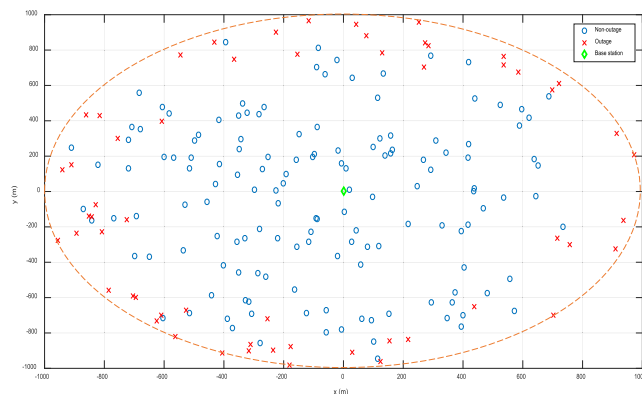
**FIGURE 27.** The comparison of the outage and the non-outage distributions for the proposed approach and the conventional method after the 2nd rebroadcast.

In Figure 26(a), the success rate is 95%. This indicates that most users can successfully receive the emergency information as text information and/or image information in the cell even within two broadcasts (one broadcast and one rebroadcast). This also reveals that most users can rapidly react to emergencies in the cell. Figure 26(b) exhibits the outage and the non-outage distributions for the conventional method after the 1st rebroadcast. The success rate is just 64% in Figure 26(b). In the conventional case, 36% of the users still fail in receiving the emergency information in the cell even after the rebroadcast.

Figure 27 exhibits the comparison of the outage and the non-outage distributions for the proposed approach and the conventional method after the 2nd rebroadcast. Figure 27(a) shows the outage and the non-outage distributions for the proposed method after the 2nd rebroadcast. In Figure 27(a), the success rate is 99.5%. This indicates that almost all the users can successfully receive the emergency information as text information and/or image information in the cell within three broadcasts (one broadcast and two rebroadcasts). This also reveals that almost all the users can react to emergencies in the cell within three broadcasts. Figure 27(b) exhibits the outage and the non-outage distributions for the conventional



(a)



(b)

**FIGURE 28.** The comparison of the outage and the non-outage distributions for the proposed approach and the conventional method after the 3rd rebroadcast.

method after the 2nd rebroadcast. The success rate is just 69% in Figure 27(b). In the conventional case, 31% of the users still fail in receiving the emergency information in the cell even after three broadcasts. Therefore, lots of users have difficulties in reacting to emergencies in the conventional case. The comparison of Figures 25 and 27 reveals that the success rate increases considerably (from 58.5% to 99.5%) in the proposed case. The comparison also reveals that the success rate increases a little (from 58.5% to 69%) in the conventional case. This indicates that the novel rebroadcast mechanism is much superior to the conventional carousel mechanism.

Figure 28 exhibits the comparison of the outage and the non-outage distributions for the proposed approach and the conventional method after the 3rd rebroadcast. Figure 28(a) shows the non-outage distribution for the proposed method after the 3rd rebroadcast. In Figure 28(a), the success rate is 100%. This indicates that all users can successfully receive the emergency information as text information and/or image information in the cell within four broadcasts (one broadcast and three rebroadcasts). This also reveals that all users can react to emergencies in the cell within four broadcasts. Figure 28(b) exhibits the outage and

the non-outage distributions for the conventional method after the 3rd rebroadcast. The success rate is just 71.5% in Figure 28(b). In the conventional case, almost 30% of the users still fail in receiving the emergency information in the cell even after four broadcasts. Moreover, the success rate does not increase noticeably as the number of rebroadcasts increases in the conventional case. Even after many rebroadcasts, it is likely that lots of users still have difficulties in reacting to emergencies. Therefore, the conventional approach is not suitable for urgent emergency cases. Since the proposed approach is much superior to the conventional method in terms of latency and reliability, the presented WEA is much more suitable for urgent emergency cases.

## V. CONCLUSION

This paper presents a novel WEA technique in 5G cellular systems, which overcomes the drawbacks (latency and reliability) of the conventional WEA. The novel WEA approach is based on the image code and the cell clustering. The cell clustering also offers the cell diversity.

In order to enhance the latency performance, the proposed WEA approach delivers the image-code information for rebroadcasts. The novel WEA method effectively exploits the feature of the 5G CBS message structure for the embedding of the image code. Therefore, the embedded image code never sacrifices the maximum number of text characters. Since the length of image code is much smaller than that of text characters in the 5G CBS message, the image-code delivery significantly contributes to the enhancement of the latency performance. Furthermore, the image-code delivery is very useful for illiterate persons or foreigners.

In order to enhance the reliability performance, the novel WEA technique exploits the proposed cell clustering, which gives the cell diversity. The cell clustering consists of initial clustering and adaptive clustering. Since the base station can track the mobile terminals in the cell, it determines the potential outage terminals for the initial clustering. Then, the base station finds the 1st initial clusters (which include the potential outages) using the  $K$ -means algorithm. Finally, the base station associates the potential non-outages to the corresponding 1st initial cluster, which completes the initial clustering procedure. The adaptive clustering is initiated after the base station broadcasts the CBS alert message. For the adaptive clustering, the selected non-outages exploit the cell diversity in order to rebroadcast the image-code information in each cluster. The adaptive clustering continues until the number of outages is zero in each cluster. In the adaptive clustering, the presented cell diversity is equivalent to the MRC diversity technique. Since the MRC diversity method guarantees the optimal performance, the proposed cell diversity can considerably improve the reliability performance.

Experimental evaluation reveals the effectiveness of the proposed WEA approach in 5G cellular systems. The latency evaluation indicates that the proposed image-code delivery is superior to the conventional text-message delivery. The BER evaluation reveals the superiority of the proposed

cell diversity. Furthermore, the evaluation confirms that the cell diversity can offer the optimal performance. The placement results exhibit that the proposed WEA approach outperforms the conventional WEA method in terms of latency and reliability. Finally, the experimental results confirm that the proposed approach is more suitable for emergency alert services especially in the cases of urgent emergencies. Furthermore, the proposed method is very suitable for illiterate persons or foreigners.

Note that the proposed approach can support the 5G URLLC. The URLLC system is not directly related with the CBS. Nonetheless, we can extend the CBS scope to include the URLLC devices. If a 5G base station broadcasts an emergency code (which is like the proposed image code) to URLLC devices in the cell, the devices can react to the emergency code and do the following tasks:

- The URLLC devices automatically close house windows, gas valves, and garage gates if the emergency code indicates tornado or hurricane. This is an emergency alert system for smart home.
- The URLLC devices automatically terminate any dangerous factory job if the emergency code indicates earthquake. This is an emergency alert system for smart factory.
- The URLLC devices automatically disable any elevator facility if the emergency code indicates earthquake. This is an emergency alert system for smart building.

For the 5G CBS approach based on URLLC, the URLLC devices should employ a decoding module for the data structure of SIB 8 [15].

For a high-depth evaluation including message-efficacy improvement and immediate reactivity, we have to make a benefit analysis for the proposed emergency alert system [28], [29]. Note that we need to get real data (including survey data) from a real-time emergency alert system for the benefit analysis. Since it is not easy to get real data currently, we leave the high-depth evaluation as future work.

## REFERENCES

- [1] F. Wang, Z. Pei, L. Dong, and J. Ma, "Emergency resource allocation for multi-period post-disaster using multi-objective cellular genetic algorithm," *IEEE Access*, vol. 8, pp. 82255–82265, 2020.
- [2] E. Gunduzhan, B. Doshi, and L. Benmohamed, "Wireless emergency alerts in arbitrary sized target areas: Mobile location aware emergency notification," in *Proc. IEEE Mil. Commun. Conf.*, Oct. 2015, pp. 1606–1611.
- [3] W. Luplow and J. Kutzner, "Emergency alerts to people on-the-go via terrestrial broadcasting: The M-EAS system," in *Proc. IEEE Int. Conf. Technol. Homeland Secur.*, Nov. 2013, pp. 779–783.
- [4] V. Javidroozi, H. Shah, and G. Feldman, "Urban computing and smart cities: Towards changing city processes by applying enterprise systems integration practices," *IEEE Access*, vol. 7, pp. 108023–108034, 2019.
- [5] *Study for Requirements for a Public Warning System (PWS) Service*, document 3GPP TR 22.968, Release 16, Jul. 2020.
- [6] A. Sengupta, A. R. Alvarino, A. Catovic, and L. Casaccia, "Cellular terrestrial broadcast—Physical layer evolution from 3GPP release 9 to release 16," *IEEE Trans. Broadcast.*, vol. 66, no. 2, pp. 459–470, Jun. 2020.
- [7] D. Chang, L. Cui, and Z. Huang, "A cellular-automaton agent-hybrid model for emergency evacuation of people in public places," *IEEE Access*, vol. 8, pp. 79541–79551, 2020.

- [8] H. Elsawy, W. Dai, M. Alouini, and M. Z. Win, "Base station ordering for emergency call localization in ultra-dense cellular networks," *IEEE Access*, vol. 6, pp. 301–315, 2017.
- [9] *Technical Realization of Cell Broadcast Service (CBS)*, document 3GPP TS 23.041, Version 16.2.0, Release 16, Dec. 2019.
- [10] *Wireless Emergency Alert (WEA) 3.0 Via 5G Public Warning System Specification*, Standard ATIS-0700043, 2020.
- [11] *Feasibility Study for WEA Supplemental Text*, Standard ATIS-0700026, Dec. 2015.
- [12] A. Ghosh, A. Maeder, M. Baker, and D. Chandramouli, "5G evolution: A view on 5G cellular technology beyond 3GPP release 15," *IEEE Access*, vol. 7, pp. 127639–127651, 2019.
- [13] *Feasibility Study of LTE WEA Message Length*, Standard ATIS-0700023, Oct. 2015.
- [14] *5G System; Technical Realization of Service Based Architecture; Stage 3*, document 3GPP TS 29.500, Version 16.5.0, Release 16, Sep. 2020.
- [15] *Radio Resource Control (RRC) Protocol Specification*, document 3GPP TS 38.331, Version 15.8.0, Release 15, Dec. 2019.
- [16] *Alphabets and Language-Specific Information*, document 3GPP TS 23.038, Version 16.0.0, Release 16, Jul. 2020.
- [17] K. P. Sinaga and M.-S. Yang, "Unsupervised  $K$ -means clustering algorithm," *IEEE Access*, vol. 8, pp. 80716–80727, 2020.
- [18] T. Li, F. Yang, D. Zhang, and L. Zhai, "Computation scheduling of multi-access edge networks based on the artificial fish swarm algorithm," *IEEE Access*, vol. 9, pp. 74674–74683, 2021.
- [19] A. Goldsmith, *Wireless Communications*. Cambridge, U.K.: Cambridge Univ. Press, 2005.
- [20] S. Chang, "An emergence alert broadcast based on cluster diversity for autonomous vehicles in indoor environments," *IEEE Access*, vol. 8, pp. 84385–84395, 2020.
- [21] G. Kongara, C. He, L. Yang, and J. Armstrong, "A comparison of CP-OFDM, PCC-OFDM and UFMC for 5G uplink communications," *IEEE Access*, vol. 7, pp. 157574–157594, 2019.
- [22] *Part 11: Wireless LAN Medium Access Control(MAC) and Physical Layer(PHY) Specifications*, IEEE Standard 802.11p, 2010.
- [23] A. Al-Rimawi, J. Siam, A. Abdo, and D. Dardari, "Performance analysis of dynamic downlink PPP cellular networks over generalized fading channels with MRC diversity," *IEEE Access*, vol. 9, pp. 39019–39027, 2021.
- [24] I. Marsic, *Computer Networks: Performance and Quality of Service*. New Brunswick, NJ, USA: Rutgers, 2013.
- [25] J. G. Proakis, *Digital Communications*, 4th ed. New York, NY, USA: McGraw-Hill, 2001.
- [26] A. Hikmaturokhman, M. Suryanegara, and K. Ramli, "A comparative analysis of 5G channel model with varied frequency: A case study in Jakarta," in *Proc. Int. Conf. Smart Comput. Commun.*, Jun. 2019, pp. 1–5.
- [27] Y. Byun, H. Lee, S. Chang, S. J. Choi, and K. Pyo, "A method of image display on cellular broadcast service," *J. Broadcast Eng.*, vol. 25, no. 3, pp. 399–404, May 2020.
- [28] F. Pappenberger, H. L. Cloke, D. J. Parker, F. Wetterhall, D. S. Richardson, and J. Thielen, "The monetary benefit of early flood warnings in Europe," *Environ. Sci. Policy*, vol. 51, pp. 278–291, Aug. 2015.
- [29] T. J. Teisberg and R. F. Weiber, "Background paper on the benefits and costs of early warning systems for major natural hazards," World Bank Group, Global Facility Disaster Reduction Recovery, Washington, DC, USA, 2009.



**SEKCHIN CHANG** received the B.S.E.E. and M.S.E.E. degrees from the Department of Electronics and Computer Engineering, Korea University, Seoul, South Korea, in 1991 and 1993, respectively, and the Ph.D. degree from the Department of Electrical and Computer Engineering, The University of Texas at Austin, in 2001. From 1993 to 1998, he was with the Electronics and Telecommunications Research Institute (ETRI), Daejeon, South Korea. He was also with Motorola, Inc., Austin, TX, USA, from 2000 to 2004. Since February 2004, he has been with the Department of Electrical and Computer Engineering, University of Seoul, Seoul, where he is currently a Full Professor. His current research interests include wireless emergency alert systems, the Internet-of-Things, real-time locating systems, embedded vehicle systems, and wireless communications.

• • •